Polymer-ceramic composite cathode with enhanced storage capacity manufactured by field-assisted sintering and infiltration

Martin Ihrig[1,2,], Ruijie Ye[1], Alexander M. Laptev[1†], Daniel Grüner[3], Rayan Guerdelli[4], Walter-Sebastian Scheld[1], Martin Finsterbusch[1,4], Hans-Dieter Wiemhöfer[4], Dina Fattakhova-Rohlfing[1], and Olivier Guillon[1,2,4]*

[1]Institute of Energy and Climate Research – Materials Synthesis and Processing, Forschungszentrum Jülich GmbH, 52425 Jülich, Germany

[2]Institute of Mineral Engineering, RWTH Aachen University, 52064 Aachen, Germany

[3]Institute of Energy and Climate Research – Microstructure and Properties of Materials, Forschungszentrum Jülich GmbH, 52425 Jülich, Germany

[4]Helmholtz Institute Münster: Ionics in Energy Storage, 48149 Münster, Germany

KEYWORDS: *polymer-ceramic cathode, garnet structure, composite cathode, field-assisted sintering, infiltration, low impedance, enhanced storage capacity*

ABSTRACT: Polymer-ceramic all-solid-state Li batteries (ASSLBs) combine the advantages of fully inorganic and polymer-based ASSLBs. In particular, the application of proposed polymer-ceramic composite cathodes could be essential for enhancement of ASSLBs energy storage capacity. The use of modified Field-Assisted Sintering Technique with adjustable pressure and with alternative mica foil enables fabrication of porous cathodes at reduced sintering temperature and without side phase formation. This allows sintering of porous $LiCoO_2$/$Li_7La_3Zr_2O_{12}$:Ta composite network suitable for polymer infiltration and assembly in a ASSLB from cathode side. The ceramic $LiCoO_2$/$Li_7La_3Zr_2O_{12}$:Ta composite cathodes infiltrated with ion-conducting polymer has shown an enhanced areal storage capacity.

1. INTRODUCTION

Li batteries with a solid-state electrolyte can potentially outperform conventional Li-ion batteries with liquid or polymer electrolyte.[1] This battery type is known in the literature as all-solid-state lithium batteries (ASSLBs). In ASSLBs a Li-ion-conducting ceramic, e.g. garnet-type oxide $Li_7La_3Zr_2O_{12}$ (LLZO), is typically used as electrolyte. LLZO has a wide electrochemical window, stability vs. lithium, and good ionic conductivity at room temperature.[1] The cathode in ASSLBs is manufactured from a cathode active material (CAM), such as $LiCoO_2$ (LCO). The efficiency of Li-ion storage can be enhanced by the use of composite cathode consisting from a CAM and an ion-conducting ceramic, e.g. LCO/LLZO.[2] In such a composite cathode LLZO delivers Li-ions through the bulk enhancing the volumetric loading of LCO. In the present paper the addition of an ion-conducting polymer into LCO/LLZO cathode was proposed aiming at further increase of cell performance due to facilitation of CAM usage. To the best of our knowledge, the proposed concept of polymer-ceramic cathode is new in ASSLBs architecture. At the same time, a similar approach has been applied for manufacturing of polymer-ceramic electrolytes.[3-4] They are fabricated mostly

by tape casting of slurry with polymer matrix, ceramic filler and a solvent. An alternative technology includes free sintering of tape-casted LLZO porous network and subsequent infiltration by liquid or polymer electrolyte.[5]

Free sintering of LCO/LLZO composite requires relatively high temperature and/or long sintering time. This results in loss of volatile Li with decrease in electrochemical performance.[1] In the present work the LCO/LLZO composite cathodes were manufactured in a powder-based process by Field-Assisted Sintering Technique also known as Spark Plasma Sintering (FAST/SPS). FAST/SPS enables fast heating (100°C/min and higher) and application of mechanical pressure leading to reduction in sintering temperature and time needed for fabrication of dense pellets.[6] Thereby, Li evaporation and grain growth can be significantly reduced. This technology was used in our previous papers for fabrication of half-cells with dense LLZO electrolyte and dense LCO/LLZO composite cathode.[7-8] However, the appearance of side phase after sintering at low pressure and residual porosity were observed. The reason for that was partial reduction of oxides by carbon originated from graphite foil in FAST/SPS setup. In the present paper the graphite foil was replaced by carbon-free mica foil. This measure enabled FAST/SPS sintering of porous LCO/LLZO network without side phase formation. The obtained porous skeleton was infiltrated with polymer electrolyte to fabricate a polymer-ceramic composite cathode. The cathode was assembled with an anodic half-cell consisting of dense FAST/SPS-sintered LLZO electrolyte and attached indium (In) foil used as anode. The ASSLB with polymer-ceramic composite cathode showed significantly lower impedance and remarkably higher area-specific storage capacity as compared to the similar ASSLBs with pure ceramic (porous or dense) composite cathodes. Furthermore, the functionality and the increased areal storage capacity of

proposed polymer-ceramic cathode and the advantage of related ASSLB architecture were demonstrated.

2. MATERIAL AND METHODS

FAST/SPS sintering − A Ta- and Al-substituted LLZO powder ($Li_{6.45}Al_{0.05}La_3Zr_{1.6}Ta_{0.4}O_{12}$, LLZO:Ta) was used as Li-ion-conductive constituent. The details on powder synthesis and FAST/SPS procedure can be found elsewhere.[8] In contrast to the common FAST/SPS practice all elements of the FAST/SPS setup were fabricated from molybdenum alloy (Plansee AG). Additionally, in the present work, graphite foil in FAST/SPS setup was replaced by mica foil. Thus, the reactions between LCO/LLZO:Ta and graphite and the side phase formation were omitted. A sintering temperature of 675°C and a dwell time of 10 min were applied during all FAST/SPS cycles. The applied pressure varied in the range between 50 MPa and 440 MPa to prepare an LCO/LLZO:Ta (1:1 wt.-ratio) network (composite cathode) with different porosity. Dense LLZO:Ta separators were manufactured as described elsewhere.[7-8] After FAST/SPS sintering, the pellet surface was polished by sandpaper. The details of material and structural characterization are presented in the Supporting Information part.

ASSLB fabrication − A sintered porous LCO/LLZO:Ta sample with a diameter of 12 mm, a thickness of 160 µm and with a residual porosity of 20% was sputter-coated with Au (Cressington 108) for 150 s (~5 nm) on one side to obtain a current collector. Afterwards, the sample was placed in an Ar-filled glove box and covered on the un-sputtered side with a dissolved polymer electrolyte. As the ion-conducting polymer, a solution of poly(bis(2-(2-methoxyethoxy)ethoxy)phosphazene) denoted as MEEP and $LiB(C_2O_4)_2$ salt in acetonitrile was used. The MEEP is stable up to 5.0 V vs Li/Li^+ and shows a high ionic conductivity of around 2.5 mS cm^{-2} at 30°C.[9] The sample was dried at 80°C for 60 min and polymerized under UV light (UV

cube 100, Hönle Group) for 30 min. The LCO/LLZO:Ta sample infiltrated by MEEP polymer was used as a polymer-ceramic composite cathode. The anodic half-cell consisted of a dense FAST/SPS-sintered LLZO:Ta separator Au-sputtered for 30 s (~1 nm) on the anode side and a mechanically attached indium foil served as anode. Before attaching to the composite cathode, the LLZO:Ta side of the half-cell was covered with the MEEP as described above. The assembled polymer-ceramic cell was placed into a Swagelok cell and sealed. The sketch of the polymer-ceramic cell is presented in Figure 1.

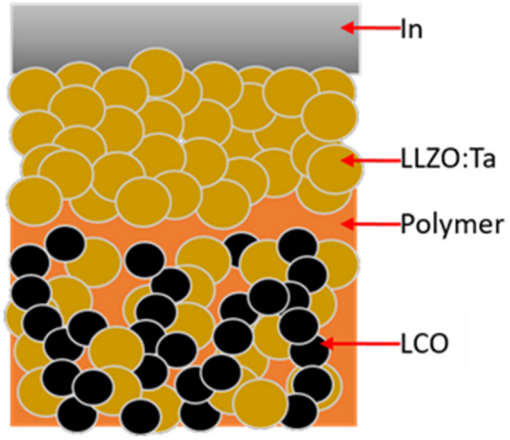

Figure 1. Sketch of polymer-ceramic cell consisting of porous LCO/LLZO composite cathode infiltrated by polymer and half-cell with LLZO:Ta separator and In anode.

Electrochemical characterization − The ASSLBs were loaded into a climate chamber VT 4002EMC (Vötsch). The electrochemical characterization was performed at 80°C using a BioLogic VMP-300 potentiostat. Electrochemical impedance spectroscopy (EIS) was studied in the frequency range from 3 MHz to 1 Hz in a perturbation field with an amplitude of 10 mV. The impedance spectra were fitted using the ZView software (Scribner). The cycling was performed using the constant-current-constant-voltage (CC-CV) charging. The cells were charged to 3.4 V vs. In-Li (i.e. 4.0 V vs. Li/Li^+) with a constant current density of 50 μA cm^{-2} and held at a voltage

of 3.4 V until the current density dropped to 10 μA cm^{-2}. Discharge of the batteries was done with a constant current density of 50 μA cm^{-2} until the voltage reduced to 2.8 V.

3. RESULTS AND DISCUSSION

Conventional free sintering of LCO/LLZO composite cathodes faces the challenge of elemental inter-diffusion between LCO and LLZO and formation of low-conductive side phases due to relatively high sintering temperature and long dwell time. The formation of side phases leads to enhanced impedance and reduced electrochemical performance.[1] Recently, we reported the successful co-sintering of an LCO and LLZO:Ta powder mixture via high-pressure FAST/SPS technique.[7-8] The application of high pressure (440 MPa) during FAST/SPS sintering suppressed diffusion of carbon (originated from graphite foil) into cathode bulk and its reaction with LCO and LLZO:Ta which is crucial for the phase purity (Figure 2). However, the application of high pressure leads to nearly full densification of sintered cathode (a porosity of around 5 %, Figure 3a) with closed pores (SI: Figure S1). Thus, the infiltration of cathode with polymer is not possible.

The replacement of graphite foil by alternative mica foil in FAST/SPS setup, as proposed in this work, enabled sintering at lower pressures without formation of side phases such as $La_2Li_{1-x}Co_xO_4$ (27° and 32°) and CoO (36° and 42°) in Figure 2, apparently caused by reaction of LLZO:Ta and/or LCO with carbon.[9] Thus, the carbon diffusion into bulk can be suppressed either by rapid densification with application of high pressure or/and by application of non-graphite tooling.

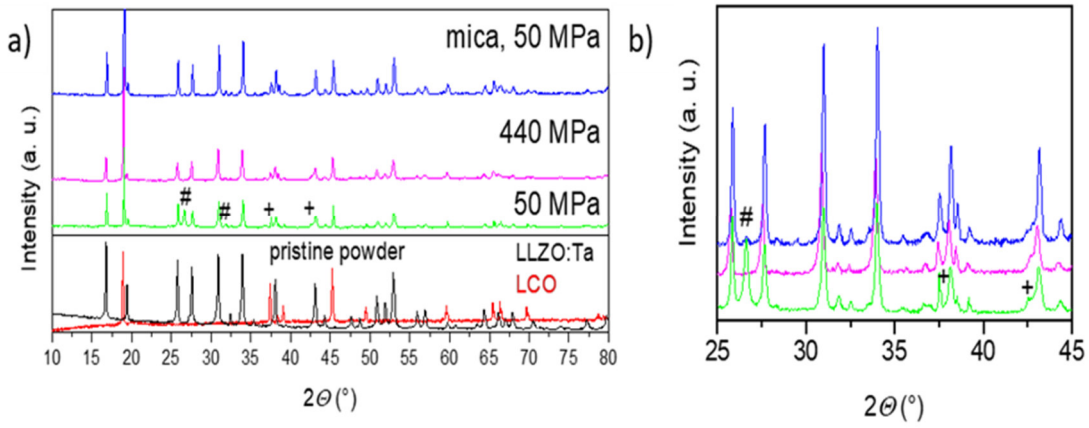

Figure 2. XRD patterns of LCO/LLZO:Ta composite cathode sintered by FAST/SPS (675°C for 10 min, Ar) at various pressure with graphite foil (green and pink) and with mica foil (blue). The side phase peaks are marked with # for $La_2Li_{1-x}Co_xO_4$ and with + for CoO.

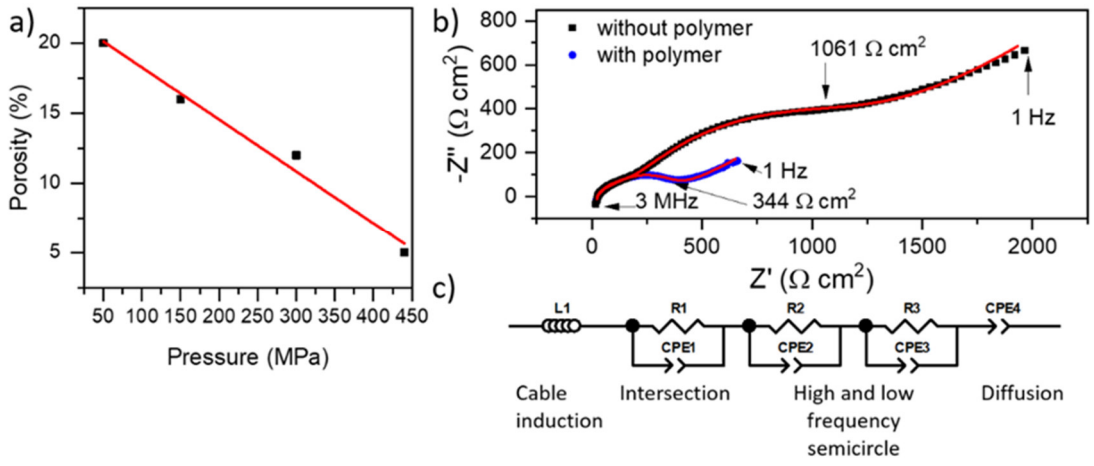

Figure 3. (a) Porosity of FAST/SPS sintered LCO/LLZO:Ta composite cathode vs. applied mechanical pressure. (b) EIS spectra of batteries with porous (20%) non-infiltrated and polymer-infiltrated composite cathode. (c) Equivalent circuit used for fitting (L: inductor, R: ohmic resistors, CPE: Constant Phase Elements).

As the mechanical pressure in FAST/SPS cycle can be independently varied, the tuning of cathode porosity becomes possible. At the same time, a minimal pressure of 50 MPa is required to

obtain a mechanically stable composite cathode. The resulting porosity of sintered composite cathodes varied between 5% and 20% depending on applied FAST/SPS pressure (Figure 3a). This allowed the adjustment of porosity in a way enabling good infiltration of sintered porous network. A total porosity of above 10% was required to ensure open porosity sufficient for infiltration.

In principle, the FAST/SPS technique enables sintering of composite cathode and LLZO:Ta separator in one step.[7-8] However, at a low FAST/SPS pressure (e.g. 50 MPa) the LLZO:Ta separator will be porous. This could lead to its penetration by Li dendrites and to short circuit in the cell. Therefore, the composite cathode has to be either sintered on a dense separator or attached to a dense sintered separator e.g. using a layer of conductive polymer. In this work, the polymer-ceramic ASSLB was prepared by attaching of the infiltrated composite cathode to the dense LLZO:Ta separator through a MEEP layer served as a kind of "glue" (Figure 1).

The first In │ LLZO:Ta │ LCO/LLZO:Ta full cell was assembled by attachment of In anode. To highlight the influence of polymer infiltration on total impedance, the second fully inorganic (without MEEP infiltration and without MEEP layer) LLZO:Ta │ LCO/LLZO:Ta half-cell was fabricated with one-step FAST/SPS low-pressure (50 MPa) sintering. Thus, both LCO/LLZO:Ta cathode and LLZO:Ta separator in such a half-cell were porous. Then the In anode was attached. In general, the porosity of LLZO:Ta separator within investigated range (up to 20%) does not impact significantly the ionic conductivity. In particular, the ionic conductivity of LLZO:Ta pellets with 8% and 20% porosity was measured by EIS at room temperature. Their ionic conductivity was comparable with a value of around 0.2 mS cm^{-1} (SI: Figure S2). Therefore, the comparison of impedance for fully inorganic (porous separator, non-infiltrated cathode) and polymer-ceramic (dense separator, infiltrated cathode) ASSLBs is possible. The results of impedance measurement for two full cells are presented in Figure 3b. Both EIS spectra have a high-frequency intersection

with the x-axis, a semicircle at high and medium frequencies and a low frequencies Li-ion diffusion tail. Similar spectra were earlier observed for the nearly dense (a porosity of 5%) composite cathodes prepared by FAST/SPS.[8] The EIS spectra were fitted with an equivalent circuit shown in Figure 3c. However, the fitted capacities did not match either the expected values for single interfaces (LCO/LLZO:Ta, LCO/MEEP, LLZO:Ta/MEEP) nor the typical values for grain boundaries (SI: Tab. S1).[10] Thus, only the intersection at high frequency might give an indication of the bulk impedance of LLZO:Ta with 22 Ω cm^2.[11] Therefore, merely the total impedances of fully inorganic and polymer-ceramic ASSLBs can be reasonable evaluated and compared. The total impedance reduced from 1061 Ω cm^2 for the fully inorganic ASSLB to 344 Ω cm^2 for the polymer-ceramic ASSLB evidencing the positive effect of cathode infiltration (Figure 3b). The significantly lower total impedance for the polymer-ceramic ASSLB indicates that a continuous Li-ion conduction pathway in the fully ceramic ASSLB was not formed although that this could be expected.[3-4] Thus, the ionic conductivity of solid ion-conducting phase in a composite cathode can be significantly improved by infiltration with MEEP polymer. Besides, the LCO/MEEP interface might have lower impedance than the LCO/LLZO:Ta interface.

With a total volumetric amount of 20% the pores appeared as interconnected and homogeneously distributed throughout the entire composite cathode, allowing proper infiltration with MEEP (Figure 4a). This was confirmed by EDX mapping of carbon as presented in Figure 4b. The infiltration of the composite cathode by MEEP polymer enabled cycling of the polymer-ceramic ASSLB (Figure 4c) while the fully inorganic ASSLB (with porous cathode and porous electrolyte) immediately jumped to 3.4 V without charging. This behavior is most likely related to the high impedance of such a cell (SI: Figure S3). In general, a large thickness of composite cathodes can lead to reduced electronic and ionic conductivity limiting cycling ability and reduced storage

capacity. With thinning of composite cathode these limitations should be less pronounced with better cycling. However, the area-specific storage capacity thereby decreases.[12]

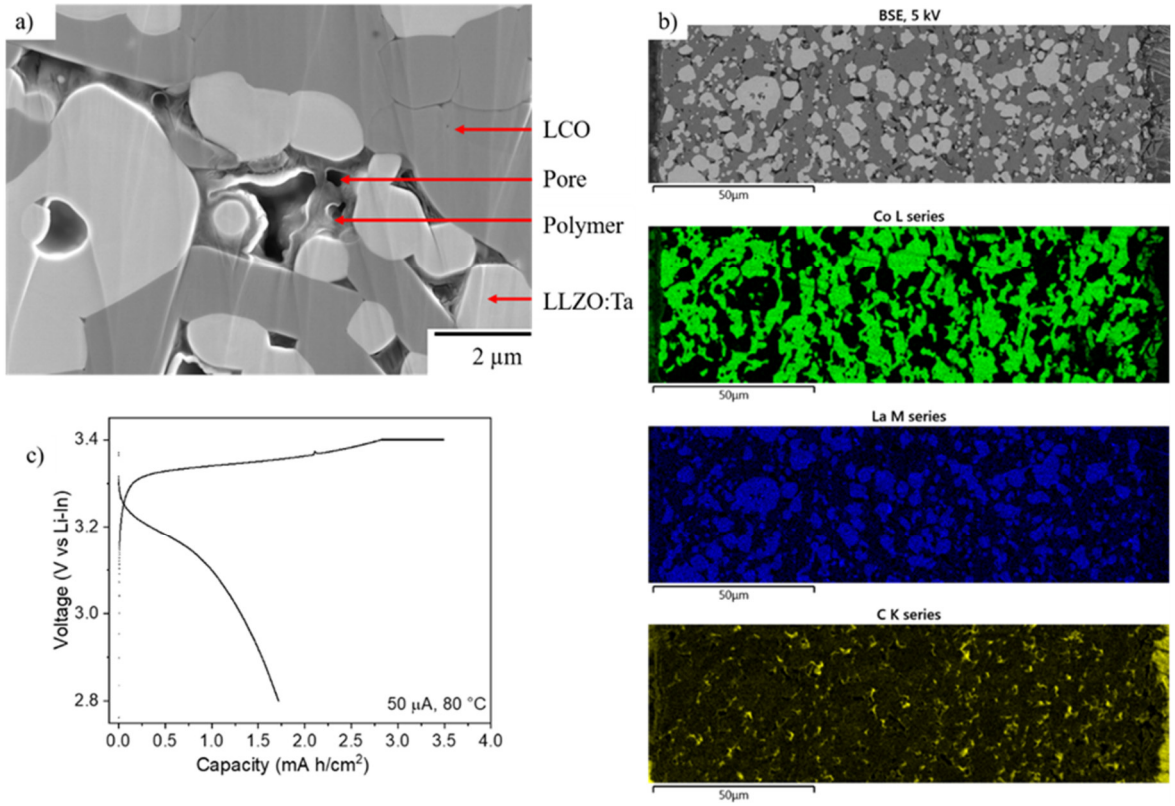

Figure 4. (a) Cross-section of composite cathode with an initial porosity of 20% infiltrated by MEEP. (b) SEM image of composite cathode with EDX mapping for Co (green), La (blue), and carbon (yellow) showing distribution of LCO, LLZO and MEEP. (c) Charge and discharge of a polymer-ceramic cell.

The infiltrated composite cathode provided a high initial area-specific charge capacity of 3.4 mA·h·cm^{-2} with 64% LCO utilization, although the ASSLB was still not fully charged in order to prevent cracking of LCO/LLZO:Ta interface due to volume change of LCO[13] The high LCO utilization indicates that the bulk of composite cathode is well-accessible for Li-ions. This means that LLZO:Ta and MEEP formed a Li-ion conducting network percolating the cathode bulk. Thus,

the effective use of thick composite cathode resulting in high area-specific capacity becomes possible. The first discharge provided a specific-area storage capacity of around 1.8 mA h cm^{-2}. The lower discharge capacity in comparison with the charge capacity is typically observed in ASSLBs, especially when an In anode is used, as some Li atoms could be trapped within the Li-In alloy.[12] The obtained initial charge and discharge energy are comparable with performance of regular fully inorganic ASSLBs for which a highest specific-area storage capacity of 1.6 mA h cm^{-2} is reported.[12] Thus, even the first prototype of the ASSLB with polymer-ceramic cathode demonstrates the good prospect for proposed concept of batteries with polymer-ceramic composite cathode. In particular, the gravimetric and volumetric storage capacities were around 94 $mA{\cdot}h{\cdot}g^{-1}$ and 212 $mA{\cdot}h{\cdot}cm^{-3}$, which is comparable with fully dense LCO/LLZO:Ta composite cathodes (94 $mA{\cdot}h{\cdot}g^{-1}$ and 218 $mA{\cdot}h{\cdot}cm^{-3}$).[8] The promising aspect for the polymer-ceramic battery is that the gravimetric and volumetric storage capacity were obtained even in a thick composite cathode of 160 μm, thus reaching high total and area specific capacity.[14] Further optimization of infiltration process will be performed in order to reach even higher LCO utilization in thicker composite cathodes.

4. CONCLUSIONS

The FAST/SPS sintering under varied pressures in a metallic tool with the use of mica foil enables sintering of porous LCO/LLZO:Ta network without side phases formation. The infiltration of this network by MEEP polymer results in fabrication of a polymer-ceramic composite cathode with low impedance and enhanced energy storage capacity comparing to both non-infiltrated porous and nearly-dense composite cathodes. Thus, the proposed architecture with a polymer-ceramic cathode and a dense electrolyte joined by polymer layer is a promising concept for Li

batteries. In addition, the FAST/SPS sintering technique opens the opportunity for other CAMs such as $Li(Ni_{1-x-y}Co_xMn_y)O_2$ (NMC) or $LiNi_{0.5}Mn_{1.5}O_4$ (LNMO) to reveal the potential of polymer-ceramic Li batteries.

ASSOCIATED CONTENT

Supporting Information

The Supporting Information is available free of charge at the ACS Applied Energy Materials website.

Description of material characterization, an SEM image of a dense composite cathode, the Nyquist plots for non-infiltrated LLZO:Ta separator with different porosity, cycling diagram for a pure ceramic cell with non-infiltrated porous cathode, and fitting parameters of Nyquist's plot for full-ceramic and polymer-ceramic battery

AUTHOR INFORMATION

Corresponding Author

Martin Ihrig – *Institute of Energy and Climate Research – Materials Synthesis and Processing, Forschungszentrum Jülich GmbH, 52425 Jülich, Germany;* Phone: +49-2461-6196841; E-mail: m.ihrig@fz-juelich.de; Fax: +49-2461-619120

Present Addresses

†**Alexander M. Laptev** is now with *Łukasiewisz Research Network - Metal Forming Institute*; 14 *Jana Pawla II St., 61-139 Poznań, Poland*

Author Contributions

The manuscript was written through contributions of all authors. All authors have given approval to the final version of the manuscript.

Notes

The authors declare no competing financial interest.

ACKNOWLEDGMENT

This work was financially supported by the German Federal Ministry of Education and Research (13XP0134A and 13XP0305A).

REFERENCES

(1) Wang, C.; Fu, K.; Kammampata, S. P.; McOwen, D. W.; Samson, A. J.; Zhang, L.; Hitz, G. T.; Nolan, A. M.; Wachsman, E. D.; Mo, Y.; Thangadurai, V.; Hu, L. Garnet-Type Solid-State Electrolytes: Materials, Interfaces, and Batteries. *Chem. Rev.* **2020**, *120 (10)*, 4257-4330. DOI: 10.1021/acs.chemrev.9b00427.

(2) Kim, K. J.; Rupp, J. L. M. All Ceramic Cathode Composite Design and Manufacturing towards Low Interfacial Resistance for Garnet-Based Solid-State Lithium Batteries. *Energy Environ. Sci.* **2020**, *13 (12)*, 4930-4945. DOI: 10.1039/d0ee02062a.

(3) Yu, X.; Manthiram, A. A. Review of Composite Polymer-Ceramic Electrolytes for Lithium Batteries. *Energy Storage Mater.* **2021**, *34*, 282-300. DOI: 10.1016/j.ensm.2020.10.006.

(4) Horowitz, Y.; Lifshitz, M.; Greenbaum, A.; Feldman, Y.; Greenbaum, S.; Sokolov, A. P.; Golodnitsky, D. Review—Polymer/Ceramic Interface Barriers: The Fundamental Challenge for Advancing Composite Solid Electrolytes for Li-Ion Batteries. *J. Electrochem. Soc.* **2020**, *167 (16)*, 160514. DOI: 10.1149/1945-7111/abcd12.

(5) Lu, W.; Xue, M.; Zhang, C. Modified $Li_7La_3Zr_2O_{12}$ (LLZO) and LLZO-Polymer Composites for Solid-State Lithium Batteries. *Energy Storage Mater.* **2021**, *39*, 108-129. DOI: 10.1016/j.ensm.2021.04.016.

(6) Bram, M.; Laptev, A.; Prasad Mishra, T.; Nur, K.; Kindelmann, M.; Ihrig, M.; Pereira da Silva, J.; Steinert, R.; Buchkremer, H.-P.; Litnovsky, A.; Klein, F.; Gonzalez-Julian, J.; Guillon, O. Application of Electric Current Assisted Sintering Techniques for the Processing of Advanced Materials. *Adv. Eng. Mater.* **2020**, *22* (6), 2000051. DOI: 10.1002/adem.202000051.

(7) Laptev, A. M.; Zheng, H.; Bram, M.; Finsterbusch, M.; Guillon, O. High-Pressure Field Assisted Sintering of Half-Cell for All-Solid-State Battery. *Mater. Lett.* **2019**, *247*, 155-158. DOI: 10.1016/j.matlet.2019.03.109.

(8) Ihrig, M.; Finsterbusch, M.; Tsai, C.-L.; Laptev, A. M.; Tu, C.-H.; Bram, M.; Sohn, Y. J.; Ye, R.; Sevinc, S.; Lin, S.-K.; Fattakhova-Rohlfing, D.; Guillon, O. Low Temperature Sintering of Fully Inorganic All-Solid-State Batteries – Impact of Interfaces on Full Cell Performance. *J. Power Sources* **2021**, *482*, 228905. DOI: 10.1016/j.jpowsour.2020.228905.

(9) Jankowsky, S.; Hiller, M. M.; Fromm, O.; Winter, M.; Wiemhöfer, H. D. Enhanced Lithium-Ion Transport in Polyphosphazene based Gel Polymer Electrolytes. *Electrochim. Acta* **2015**, *155*, 364-371. DOI: 10.1016/j.electacta.2014.12.123.

(10) Irvine, J. T. S.; Sinclair, D. C.; West, A. R. Electroceramics: Characterization by Impedance Spectroscopy. *Adv. Mater.* **1990**, 2 (3), 132-138. DOI: 10.1002/adma.19900020304.

(11) Zhang, W.; Weber, D. A.; Weigand, H.; Arlt, T.; Manke, I.; Schröder, D.; Koerver, R.; Leichtweiss, T.; Hartmann, P.; Zeier, W. G.; Janek, J. Interfacial Processes and Influence of

Composite Cathode Microstructure Controlling the Performance of All-Solid-State Lithium Batteries. *ACS Appl. Mater. Interfaces* **2017**, *9 (21)*, 17835-17845. DOI: 10.1021/acsami.7b01137.

(12) Tsai, C.-L.; Ma, Q.; Dellen, C.; Lobe, S.; Vondahlen, F.; Windmüller, A.; Grüner, D.; Zheng, H.; Uhlenbruck, S.; Finsterbusch, M.; Tietz, F.; Fattakhova-Rohlfing, D.; Buchkremer, H. P.; Guillon, O. A Garnet Structure-Based All-Solid-State Li Battery without Interface Modification: Resolving Incompatibility Issues on Positive Electrodes. *Sustain. Energy Fuels* **2019,** (1), 280-291. DOI: 10.1039/C8SE00436F.

13) Koerver, R.; Zhang, W.; de Biasi, L.; Schweidler, S.; Kondrakov, A. O.; Kolling, S.; Brezesinski, T.; Hartmann, P.; Zeier, W. G.; Janek, J. Chemo-Mechanical Expansion of Lithium Electrode Materials – On the Route to Mechanically Optimized All-Solid-State Batteries. *Energy Environ. Sci.* **2018**, *11 (8)*, 2142-2158. DOI: 10.1039/C8EE00907D.

(14) Li, Y.; Chen, X.; Dolocan, A.; Cui, Z.; Xin, S.; Xue, L.; Xu, H.; Park, K.; Goodenough, J. B. Garnet Electrolyte with an Ultralow Interfacial Resistance for Li-Metal Batteries. *J Am Chem Soc* **2018**, *140 (20)*, 6448-6455. DOI: 10.1021/jacs.8b03106.

Graphical abstract: